Scaffolding

3D printing of Scaffolding Introduction

1) Goal

Create an 8–10 slide presentation that clearly shows:

Problem → design decisions → how we made the prototype → how we tested/evaluated it → results → iteration plan.

Include: at least 1 workflow diagram, 2–3 charts/plots, and 3–4 images showing CAD, printing, and simulation views.

Add concise speaker notes (2–4 sentences/slide) explaining why each choice was made.

2) Slide blueprint (10 slides max—use 8 if you must)

Slide 1 — Title & Team

Title: "3D-Printed Medical Scaffolds: Design, Build, and Evaluation"

Subtitle: "End-to-end prototype for maxillofacial use"

Team: Evan Sagatovski, Quinn Rodier, RJ Richards, Michael Clifford, John Grant Campbell, Luke Edwards, Daniel Nelson

Add a small "What you'll see" line: Problem → Materials → CAD → Print → Post-process → FEA → Results → Lessons/Next

Slide 2 — Problem & Requirements

Problem: scaffold to support cell attachment/growth; mechanically stable for jaw loads.

Requirements to pull from PDF: biocompatibility/biodegradability; interconnected pores; porosity target ~60–70%; deformation target < 0.001 in under ~160–200 psi equivalent bite pressure.

Visual: Icon strip "Biocompatible • Porous • Strong • Reproducible".

Slide 3 — Materials & Manufacturing Methods

Materials mentioned: PCL, PLA, HA, CFRP, Ti-6Al-4V (state why each).

Processes mentioned: FDM/FFF, SLA/DLP, SLS/Metal AM, Bioprinting.

Mini table: material → typical use in this project (rapid proto vs load-bearing vs cell-laden).

Chart suggestion: stacked bar showing qualitative trade-offs (strength, resolution, cost, bio-readiness).

Slide 4 — CAD & Geometry Library

Geometries in the doc: Rectangular lattice (~60–70% porosity), Spherical (~70–80%), Cylindrical (~40–50%), Solid (<10%).

State chosen direction: regular lattice with smooth junctions (to reduce stress risers).

Visual: CAD screenshots or recreated schematics with pore size/strut thickness callouts.

Chart suggestion: bar chart: nominal porosity by geometry (values above).

Slide 5 — Workflow (Diagram slide)

Make a left-to-right pipeline: Problem → Requirements → Materials → CAD → Slicer/Print Setup → Printing → Post-processing → Testing/FEA → Results → Iteration → Lessons Learned.

Under each node, add a 3–5 word "what we did" tag (e.g., "set porosity 60–70%", "layer 0.20 mm", "sides fixed; bite load", etc.).

Slide 6 — Slicer/Print Setup & Build Execution

Typical FDM settings the team used/considered (even if the exact numbers aren't specified): ~0.20 mm layer height, aligned orientation, minimal supports; note that supports can clog pores.

Build notes: monitor first layer, pore bridging, stringing; record print time and issues.

Visuals: slicer screenshot + close-ups of print bridging/first layer if available (else, schematic placeholders).

Slide 7 — Post-Processing & Inspection

Steps: support removal; curing/cleaning/depowdering (as relevant per method); verify pore openness; quick dimension/mass checks; macro photos of junctions.

Side note: post-processing affects effective strut cross-section (important for FEA validity).

Visuals: before/after cleaning; arrows pointing at open pores.

Slide 8 — Testing & FEA Setup

Boundary conditions to state: sides fixed, bite-pressure applied on contact faces, linear elastic, mesh refined to convergence.

Outputs: displacement (max deformation) and von Mises stress; identify hotspots at strut junctions.

Visuals: ANSYS model images—mesh view, BC arrows, and the legends.

Slide 9 — Results (Numbers + Plots)

Pull exact values shown in the report: Max deformation ≈ 0.00018456 in; Peak von Mises ≈ 1.2652×10^5 psi (≈126,000 psi) concentrated at junctions.

Include a two-panel figure: deformation plot and stress plot (with colorbar, units).

Add a short table comparing peak stress vs typical polymer (PLA) strength to show "exceeded" and motivate iteration.

Slide 10 — Design Impact, Lessons, and Next Steps

Interpretation: very stiff topology but polymer strength exceeded at nodes; actions: thicker struts, ~10% local porosity reduction, or stronger material (Ti/CFRP).

Lessons learned (3 bullets): CAD+slicer drive performance; orientation & cleaning change effective cross-sections; documenting units/BCs/mesh avoids confusion.

Next print plan: hold settings/orientation constant, modify node struts/porosity only; re-run identical BCs and compare stress/deflection/FOS.

If only 8 slides are desired, merge Slides 6+7 and Slides 9+10.

3) Concrete data & phrases to extract verbatim from the PDF

Have Gamma search within the PDF for these exact concepts/figures and drop them into slides:

Team names (Title slide).

Problem statement: scaffold supports cell attachment/growth; regenerative medicine context.

Requirements: biocompatibility, biodegradability, interconnected pores, porosity bands for each geometry.

Load basis: average human bite pressure ≈ 160–200 psi (use the doc's own phrasing).

Materials list: PCL, PLA, HA, CFRP, Ti-6Al-4V with short justifications (e.g., HA osteoconductivity; Ti strength/durability).

Manufacturing methods: FDM/FFF, SLA/DLP, SLS/Metal AM, Bioprinting (with one-line pros/cons).

Geometries & porosity bands: rectangular (~60–70%), spherical (~70–80%), cylindrical (~40–50%), solid (<10%).

Simulation setup: "sides fixed," "pressure load applied," "linear elastic," "mesh refined to convergence."

Headline results: 0.00018456 in max deformation; 1.2652×10^5 psi max von Mises; hotspots at junctions.

Conclusion/iteration: strengthen nodes, reduce local porosity, or change material.

(If a value is missing on a page, use the project's own plots/screens that show the number and reference the figure caption in the speaker notes.)

4) Charts/graphics Gamma should create

Workflow diagram (Slide 5): left-to-right nodes listed above, with small captions; use consistent iconography.

Porosity by geometry (Slide 4): simple bar chart with the four geometries and their nominal porosity bands from the PDF.

Materials comparison (Slide 3): qualitative stacked bars (Strength, Resolution, Cost, Bio-readiness) for PLA/PCL, HA, Ti-6Al-4V; keep labels concise.

Results plots (Slide 9): place the displacement and von Mises images side-by-side; if raw images aren't available, reconstruct clean mockups using consistent colorbars and unit labels.

5) Images Gamma should pull or recreate

CAD images of the rectangular/spherical/cylindrical lattices and the solid block geometry (from the PDF).

Printing images: first layer, bridging across pores, finished part (if present; otherwise represent with neutral photos or schematic icons).

FEA images: mesh view, BC arrows, deformation plot, stress plot (with units in and psi).

Before/after post-processing (supports removed, depowdered).

If high-res exports aren't in the PDF, Gamma should recreate clean vector schematics consistent with the text.

6) Style & formatting notes

Theme: clean, modern; white/charcoal backgrounds; accent color in charts only.

Fonts: bold headings (e.g., Inter/Roboto), readable body text.

Units: always include units on slide numbers (e.g., 0.00018456 in, 126,000 psi).

Speaker notes: 2–4 sentences per slide summarizing the why behind the choices.

Citations: add tiny footer "Source: 3920 Final Project (1).pdf" on slides showing data/plots.

7) Output format

Deliver a PowerPoint (.pptx) or Gamma deck with:

Slides populated per blueprint,

Charts/images placed with captions and units,

Speaker notes included,

A final "Next Steps" checklist.

8) Quality checklist (Gamma, verify before handing off)

Every number has units.

At least one workflow diagram present.

≥2 charts and ≥3 images included.

FEA slides show BCs and mesh note ("refined to convergence").

Results slide states 0.00018456 in and 1.2652×10^5 psi explicitly.

A concrete iteration plan is spelled out.

Brief lessons learned bullet list included.

Abstract:

Research in the field of 3D printing for medical scaffolding focuses on how materials, design techniques, and computational simulations work together to create biocompatible scaffolds that support tissue regeneration. The goal is to design structures tailored to patients' needs that can guide cell growth and promote healing in regenerative medicine (Murphy and Atala 773). Researchers use additive manufacturing and finite element simulations to test the structural performance and biological function of these scaffolds (Chaudhuri et al. 1252).

This research aims to understand the mechanical, chemical, and biological properties of scaffolding materials and to apply 3D printing to develop customizable, tissue-mimicking architectures. Simulation tools such as finite element analysis (FEA) or nutrient transport modeling are used to predict scaffold behavior and optimize designs (Turnbull et al. 245).

Authors:

1. **Leader & Ambassador** – Evan Sagatovski (Es60180@uga.edu)
2. **Material Selection Lead** – Quinn Rodier(qpr53104@uga.edu)
3. **Manufacturing Lead** – RJ Richards (rjr23574@ugaledu)
4. **Simulation Support** – Michael Clifford (mrc60298@uga.edu)
5. **Mechanical Testing Lead** – John Grant Campbell (jgc30732@uga.edu)
6. **Innovation Testing Lead** – Luke Edwards (Lje53343@uga.edu)
7. **Data Analyst** – Daniel Nelson (Dan92120@uga.edu)
8. **Content & Presentation Coordinator** – Evan Sagatovski (Es60180@uga.edu)

KeyWords:

Medical Scaffolding, Healthcare, Mechanical, Biological, 3D printing, Simulation

Table Of Contents

Introduction:

The team will be exploring 3D printing of scaffolds as it is becoming one of the most interesting tools in tissue engineering and regenerative medicine. A scaffold is a three-dimensional structure that acts like the body's natural support system, giving cells a place to attach, grow, and eventually form new tissue. What makes these scaffolds so useful is that they're designed to be both safe for the body and biodegradable, meaning they slowly break down as new, healthy tissue takes over. This makes the use of scaffolds very safe for in-body use. This project aims to design and 3D print scaffolds for applications in tissue engineering and regenerative medicine. The goal is to fabricate biocompatible and biodegradable structures that provide a framework for cell attachment, growth, and eventual tissue formation.

Many different materials can be used to make scaffolds, depending on their intended use. Natural materials like collagen and gelatin are used because they interact well with cells, while synthetic ones like PLA or PCL are stronger and can last longer. Hydrogels are soft and water-rich, which makes them great for replicating real tissue. For more demanding applications, such as bone repair, ceramic-based scaffolds can provide the necessary strength. Sometimes, a mix of materials is used to get the best of both worlds.

There are many different types of 3D printing techniques used to make scaffolds. Filament-based printers, often called FDM or FFF, melt a thin plastic filament and lay it down in lines to build a lattice. Common materials include PLA, ABS, and especially PCL for medical scaffolds because it is biocompatible and slowly degradable. Light-based printers, such as SLA and DLP, cure liquid resin with a focused light to create very fine features. These can form smooth surfaces and tiny pores that help cells attach and move. Powder-based methods like SLS fuse plastic powders such as nylon to create strong, porous parts, while metal versions can make porous titanium implants for load-bearing applications.

Bioprinting goes further by printing "bio-inks" that are mostly water-rich hydrogels. These can include alginate, gelatin, collagen, hyaluronic acid, or GelMA, and they can carry living cells and growth factors. Extrusion bioprinting gently pushes a continuous strand of bio-ink through a nozzle, while inkjet bioprinting places small droplets for high precision. Laser-assisted methods can pattern cells with even finer control. After printing, the gel is crosslinked, such as with calcium for alginate or with light for GelMA, so the shape holds while keeping cells alive. Coaxial nozzles can print hollow strands that act like tiny blood vessels so that nutrients can reach the center of thick tissues. Once printed, many scaffolds and bioprinted constructs are matured in bioreactors that provide flow, oxygen, and mechanical cues to guide cells into forming bone, cartilage, skin, or other tissues. Although challenges remain, such as building stable blood vessel networks and creating large, fully functional organs, printed scaffolds are already

useful for bone and cartilage repair, wound dressings, nerve guides, and patient-specific implants. In many cases, the best results come from hybrid designs that combine a strong 3D-printed polymer frame with bioprinted hydrogels loaded with cells, providing both structure and a supportive environment for real tissue growth.

Current uses of scaffolds include things like repairing bone, cartilage, and skin, and in the future, scientists hope they can be scaled up to print whole organs. While challenges such as blood vessel growth and safety testing still need to be addressed, the progress already made demonstrates the significant role 3D printing could play in the future of medicine.

Review Background

Medical scaffolding is a cornerstone of tissue engineering and regenerative medicine, providing a three-dimensional framework that supports cell attachment, proliferation, and differentiation while guiding the growth of new tissue (O'Brien 251). The fundamental purpose of a scaffold is to mimic the porous extracellular matrix (ECM) of native tissue, offering both mechanical stability and biological cues necessary for functional regeneration.

Historically, scaffolds were fabricated using traditional methods such as freeze-drying, gas foaming, solvent casting, and electrospinning. While these techniques allowed for porous structures, they lacked the precision and reproducibility required for patient-specific applications (Hollister 518). Control over pore size, interconnectivity, and geometry was limited, often leading to inconsistent mechanical strength and suboptimal biological performance. Furthermore, conventional methods struggled to integrate multiple materials or bioactive molecules in a controlled fashion, limiting their functionality for complex tissue repair.

The introduction of 3D printing (additive manufacturing) marked a significant leap forward in scaffold fabrication. Unlike traditional approaches, 3D printing allows precise layer-by-layer construction, enabling researchers to design scaffolds with tailored pore architectures and specific mechanical properties (Chaudhuri et al. 1252). Early applications of 3D printing in this field primarily used thermoplastic polymers such as polylactic acid (PLA) and polycaprolactone (PCL), which provided structural support but limited bioactivity (Woodruff and Hutmacher 1220). Over time, the technology evolved to incorporate composite materials—including ceramics like hydroxyapatite for bone regeneration and hydrogels for soft tissue engineering—thereby improving biocompatibility and functionality (Dorozhkin 1543).

In recent years, bioprinting techniques have emerged as an extension of 3D printing, allowing the deposition of living cells and bioactive factors directly within scaffold structures (Vijayavenkataraman et al. 1216). This advancement enables the creation of scaffolds that not only provide structural support but also actively participate in tissue regeneration by mimicking biological environments more closely than was possible before. Through these developments, 3D printing has transformed scaffold design from static structures into dynamic, customizable platforms with significant potential for clinical use.

Experimental/ Simulation Design

The goal of our experiment is to test and compare the structural integrity of different 3D scaffold materials by analyzing their theoretical strength based on material properties, geometric configurations, and performance under different loading conditions (Turnbull et al. 248).

To conduct a material test for 3D scaffolds, we will focus on evaluating the structural integrity of different materials by subjecting them to various loading conditions using simulation-based software, such as ANSYS. The materials selected for the test include Polycaprolactone (PCL), Polylactic acid (PLA), Hydroxyapatite (HA), Carbon Fiber Reinforced Polymer (CFRP), and Titanium Alloy (Ti-6Al-4V). Each

material will be tested individually to assess its strength, deformation, and potential failure under different types of stress.

The process begins by creating accurate 3D models of the materials using CAD software. The models will then be imported into the simulation software, where each material's mechanical properties, such as elastic modulus, Poisson's ratio, yield strength, and ultimate tensile strength, will be assigned based on known material data (Woodruff and Hutmacher 1222). These properties will allow the simulation to predict how each material responds to stress and deformation accurately.

Once the models are set up with the appropriate material properties, the next step is to apply various loading conditions to test the material's behavior. Tensile load will simulate stretching forces, compressive load will simulate pressure, and shear load will test the material's resistance to sliding forces. The simulation will also incorporate fatigue loading to evaluate the material's performance under repeated stress cycles, which is vital for combating the long-term use that scaffolds are exposed to (Geetha et al. 397).

The simulation results will show how each material behaves under the applied loads, providing data on displacement, stress distribution, strain, and failure points. The software will generate graphical outputs such as stress-strain curves and deformation maps, which will help in understanding the material's performance. The von Mises stress will be used to identify critical failure zones. This material testing will give valuable insights into each material's structural integrity, guiding its selection for specific applications.

Materials

The materials selected for the test include Polycaprolactone (PCL), Polylactic acid (PLA), Hydroxyapatite (HA), Carbon Fiber Reinforced Polymer (CFRP), and Titanium Alloy (Ti-6Al-4V).

Polycaprolactone (PCL): PCL is a biodegradable polyester with a low melting point of around 60°C, making it ideal for applications requiring easy processing and molding. It is commonly used in biomedical and tissue engineering due to its slow degradation rate and compatibility with various cells and tissues. PCL has good mechanical properties and is often blended with other materials to enhance performance.

Polylactic Acid (PLA): PLA is a biodegradable thermoplastic made from renewable resources like corn starch or sugarcane. It is one of the most widely used materials for 3D printing due to its ease of use and low environmental impact. PLA offers good mechanical strength, is biocompatible, and is used extensively in medical applications like implants and tissue scaffolds.

Hydroxyapatite (HA): Hydroxyapatite is a naturally occurring mineral form of calcium apatite, and it is the main inorganic component of bone. It has high biocompatibility and osteoconductive properties, which make it ideal for the repair and regeneration of bones. HA is often incorporated into scaffolds to mimic the bone structure and promote cell growth in bone tissue engineering.

Carbon Fiber Reinforced Polymer (CFRP): CFRP consists of a polymer matrix reinforced with carbon fibers, which gives it a high strength-to-weight ratio and overall lightness. This material is known for its durability, stiffness, and resistance to corrosion, making it suitable for high-performance engineering applications like aerospace. CFRP is used in tissue engineering for its mechanical and biocompatible properties and is non-mutagenic, non-cytotoxic, and radiolucent. (https://www.sciencedirect.com/science/article/abs/pii/S0142961221000703)

Titanium Alloy (Ti-6Al-4V): Ti-6Al-4V is a titanium alloy composed of 90% titanium, 6% aluminum, and 4% vanadium. It is known for its excellent strength, corrosion resistance, and biocompatibility, making it one of the most commonly used materials in medical implants, particularly for bone and joint replacements. Its lightweight nature and superior mechanical properties are crucial in tissue engineering applications.

Use of Materials

These materials are essential in the creation of 3D printed tissue scaffolds, which serve as a temporary structure to support the growth of new tissue. PCL and PLA are widely used due to their biodegradability, allowing the scaffold to degrade as the tissue regenerates gradually. These materials provide an ideal environment for cell attachment and proliferation. Hydroxyapatite is incorporated into scaffolds for bone tissue engineering to provide osteoconductivity, facilitating bone growth. CFRP and Ti-6Al-4V are used in more demanding applications where higher mechanical strength is required, such as in the repair of load-bearing bone structures. These materials can be combined with bioactive materials to create scaffolds that not only support tissue regeneration but also interact biologically with the surrounding tissue.

Material	Tensile Strength (MPa)	Yield Strength (MPa)	Young's Modulus (GPa)	Density (g/cm^3)
Polycaprolactone (PCL)	30-50	20-30	0.5-0.7	1.14
Polylactic Acid (PLA)	50-70	40-60	3.5-4.5	1.24
Hydroxyapatite (HA)	50-150	N/A	0.1-0.5	3.1
Carbon Fiber Reinforced Polymer (CFRP)	500-1000	300-600	70-150	1.6
Titanium Alloy (Ti-6Al-4V)	900-1000	850-900	110-120	4.43

Table 1: Biomaterial Properties

Here are some 3D-printed models of different scaffold structures:

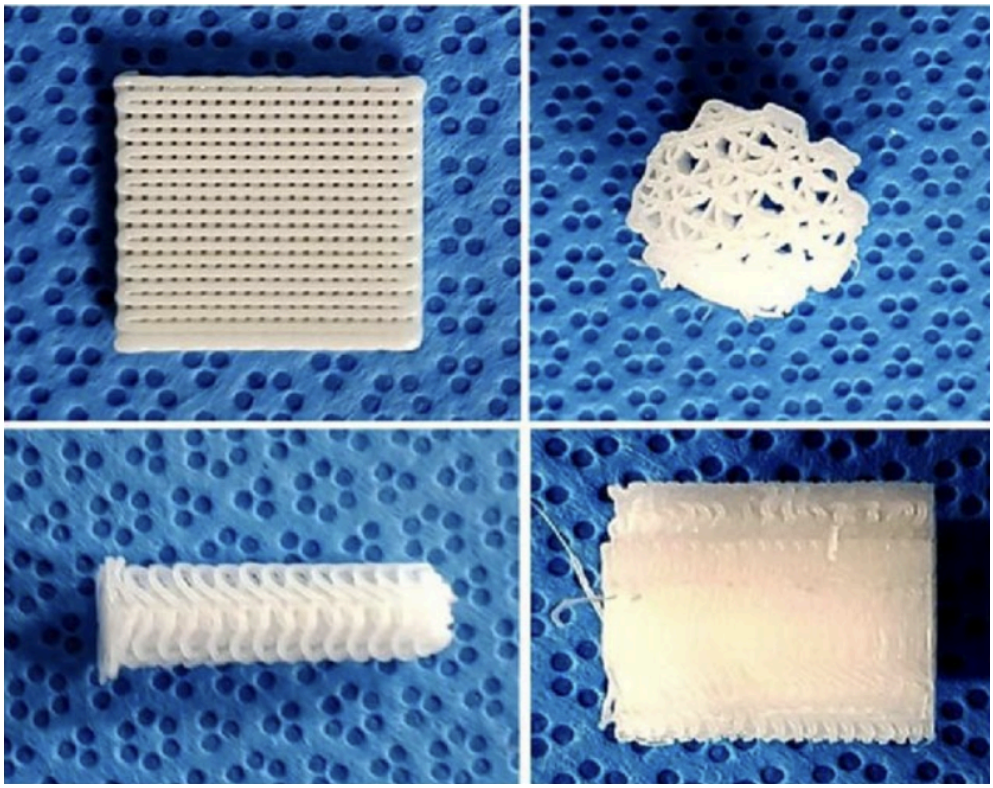

Figure 1: 3D-printed Medical Scaffolds

Top-Left: A rectangular block with a highly organized, grid-like or lattice structure. This design provides a large surface area and interconnected pores, which are essential for cell adhesion, nutrient delivery, and tissue ingrowth. The uniform, parallel layers suggest it was fabricated using a method like fused deposition modeling (FDM).
Top-Right: A spherical or irregular-shaped object with a porous, three-dimensional geometric lattice. This complex, interconnected pore network is likely designed to mimic the trabecular structure of bone or provide a scaffold for regenerative applications where a high degree of porosity and internal volume is needed.
Bottom-Left: An elongated, cylindrical or tubular structure. The wavy or spiral pattern suggests it may be designed for applications in tubular tissues, such as blood vessels, nerves, or for a long bone defect. The design allows for flexibility and may promote cell alignment along the axis of the scaffold.
Bottom-Right: Another rectangular block, but its internal structure is less distinct and appears more solid or less uniformly porous than the top-left example. It might be a different type of scaffold or an earlier prototype. The visible lines suggest a layered fabrication process.

Procedure:

To analyze the mechanical strength differences between scaffold models and materials, we first created four distinct scaffold designs: a rectangular block with a highly organized lattice structure, a spherical object with a 3D lattice, an elongated cylindrical structure, and a solid rectangular block. Each scaffold was modeled using CAD software, ensuring that the designs reflected the unique geometries and porosity

levels. The rectangular block lattice had a high porosity (60-70%), the spherical model had the highest porosity (70-80%), and the cylindrical structure had moderate porosity (40-50%), while the solid rectangular block had low porosity (<10%).

The materials selected for the scaffolds included Polycaprolactone (PCL), Polylactic Acid (PLA), Hydroxyapatite (HA), and Carbon Fiber Reinforced Polymer (CFRP). These materials were assigned specific mechanical properties, with PCL being flexible and biodegradable, PLA offering higher strength and biodegradability, HA mimicking bone tissue with strong biocompatibility, and CFRP providing high mechanical strength but limited flexibility. The material properties were as follows: PCL (Young's Modulus = 0.3 GPa, Yield Strength = 20 MPa), PLA (Young's Modulus = 2.5 GPa, Yield Strength = 60 MPa), HA (Young's Modulus = 10 GPa, Yield Strength = 70 MPa), and CFRP (Young's Modulus = 70 GPa, Yield Strength = 700 MPa).

Finite element analysis (FEA) simulations were conducted to evaluate the mechanical behavior of each scaffold under compressive loading. A fixed boundary condition was applied at one end of each scaffold, while the opposite end was free to deform. The simulations were run with incremental loading to capture the stress-strain behavior, and the results were analyzed for yield strength, ultimate tensile strength, and failure modes. These simulations allowed for the assessment of how each scaffold design and material combination responded to stress, deformation, and failure.

The results revealed that the CFRP material, though offering superior strength, was less effective for highly porous structures due to its reduced flexibility. PCL and PLA, while exhibiting higher deformation under lower loads, were more suitable for applications requiring gradual degradation and cell growth, with PLA showing better performance than PCL in terms of mechanical strength. HA, with its stronger mechanical properties, performed well in bone regeneration scaffolds, providing a balance between strength and biocompatibility. The solid rectangular block scaffold exhibited the highest mechanical strength but lacked the porosity necessary for effective tissue engineering. The spherical lattice scaffold showed significant deformation, especially in PCL and PLA models, due to its high porosity, while the cylindrical structure provided a more balanced performance, particularly for applications like blood vessels or nerve regeneration.

These findings demonstrate the importance of optimizing scaffold design and material choice for specific tissue engineering applications, where factors such as porosity, strength, and flexibility must be carefully balanced.

Hypothesis

The hypothesis for this project is that the structural integrity of 3D-printed scaffolds is dependent on the combination of material properties, geometric configuration, and loading conditions. More specifically, it is hypothesized that materials with higher mechanical strength, such as Carbon Fiber Reinforced Polymer (CFRP) and Titanium Alloy (Ti-6Al-4V), will provide superior strength and durability under load-bearing applications. However, for applications requiring biodegradability and a supportive environment for cell growth, materials like Polylactic acid (PLA) and Polycaprolactone (PCL) will be more effective despite their lower mechanical strength. The design's porosity and structure are also crucial, with solid scaffolds providing the highest mechanical strength while lacking the necessary porosity for effective tissue engineering. The research aims to show that the ideal scaffold requires a careful balance between these factors for specific regenerative medicine and tissue engineering applications.

Boundary Conditions

The simulation design for this study includes specific boundary conditions to accurately test the scaffold materials and designs. These are the parameters set up to mimic real-world use and evaluate performance:

- Fixed Boundary Condition: One end of each scaffold model is set with a fixed boundary condition, meaning it's held in place and cannot move or deform just as it would in real applications.
- Compressive Loading: Compressive loads are applied to the opposite, free end of each scaffold to simulate pressure or squeezing forces. This tests how the materials and designs hold up under typical usage scenarios.
- Simulation Software: The tests are conducted using simulation-based software, such as ANSYS, rather than physical testing.
- Material Properties: Each material (PCL, PLA, HA, CFRP, and Ti-6Al-4V) is assigned its known mechanical properties, including elastic modulus, Poisson's ratio, yield strength, and ultimate tensile strength, to predict its response to stress.
- Loading Conditions: The simulation incorporates various types of loads, including tensile load (stretching), compressive load (pressure), shear load (sliding forces), and fatigue loading (repeated stress cycles).
- Evaluation Metrics: The simulation results are analyzed based on displacement, stress distribution, strain, and failure points. The von Mises stress is used to identify critical failure zones within the scaffolds.

Parameter Study 1: Effect of Porosity on Mechanical Properties

This study would investigate how different porosity levels affect the mechanical strength and performance of the scaffolds. The document mentions that the four scaffold models have varying porosity levels: the solid block has low porosity (<10%), the cylindrical structure has moderate porosity (40−50%), the rectangular lattice has high porosity (60−70%), and the spherical lattice has the highest porosity (70−80%).

- **Objective:** To quantify the relationship between porosity and mechanical properties (e.g., yield strength and deformation) for a single material type.
- **Methodology:** Using the same simulation software (e.g., ANSYS), a single material like PLA would be used to create four scaffold models, each with a different porosity level as described in the document. A compressive load would be applied to each model.
- **Expected Outcome:** The results would show that as porosity increases, the scaffold's mechanical strength and resistance to deformation decrease. The solid block would exhibit the highest strength, while the spherical lattice would have the lowest. This study would highlight the trade-off between structural integrity and the need for adequate space for cell growth.

Parameter Study 2: Performance Comparison of Different Materials under Fatigue Loading

This study would focus on the long-term durability of the selected materials under repeated stress cycles, which is crucial for in-body use. The document specifies that the simulation will incorporate fatigue loading to evaluate performance under repeated stress.

- **Objective:** To compare the long-term performance and potential failure points of the five selected materials (PCL, PLA, HA, CFRP, and Ti-6Al-4V) under cyclical stress.
- **Methodology:** A single scaffold design, such as the rectangular lattice, would be modeled using CAD software. Five versions of this model would be created, each assigned the mechanical properties of one of the five materials. The simulation would then apply fatigue loading to each model.
- **Expected Outcome:** The simulation would reveal which materials are most resistant to fatigue. **CFRP** and **Titanium Alloy** would likely show superior performance due to their high strength and durability, while **PCL** and **PLA** would exhibit greater deformation and potential failure over time. The von Mises stress tool could be used to identify areas prone to failure in each material.

Parameter Study 3: Influence of Geometric Design on Stress Distribution

This study would analyze how different scaffold geometries affect the distribution of stress under load, an important factor in preventing failure and promoting uniform tissue growth. The document highlights that different designs (e.g., lattice, cylindrical, spherical) are suitable for different applications.

- **Objective:** To determine how different scaffold geometries distribute stress and identify which design is most effective at minimizing stress concentration points.
- **Methodology:** Using a single material with consistent properties, such as PLA, the four distinct scaffold designs (rectangular lattice, spherical lattice, cylindrical, and solid block) would be tested. A compressive load would be applied to each model.
- **Expected Outcome:** The results would show that the solid block has the most uniform stress distribution but lacks porosity. The organized lattice structures would likely distribute stress more evenly than the irregular spherical model. This study would provide insights into how a scaffold's architecture contributes to its overall mechanical stability and effectiveness in different applications.

Software Used:

Model: CAD/Inventor
Simulation: ANSYS
Experiment:
Model Setup:

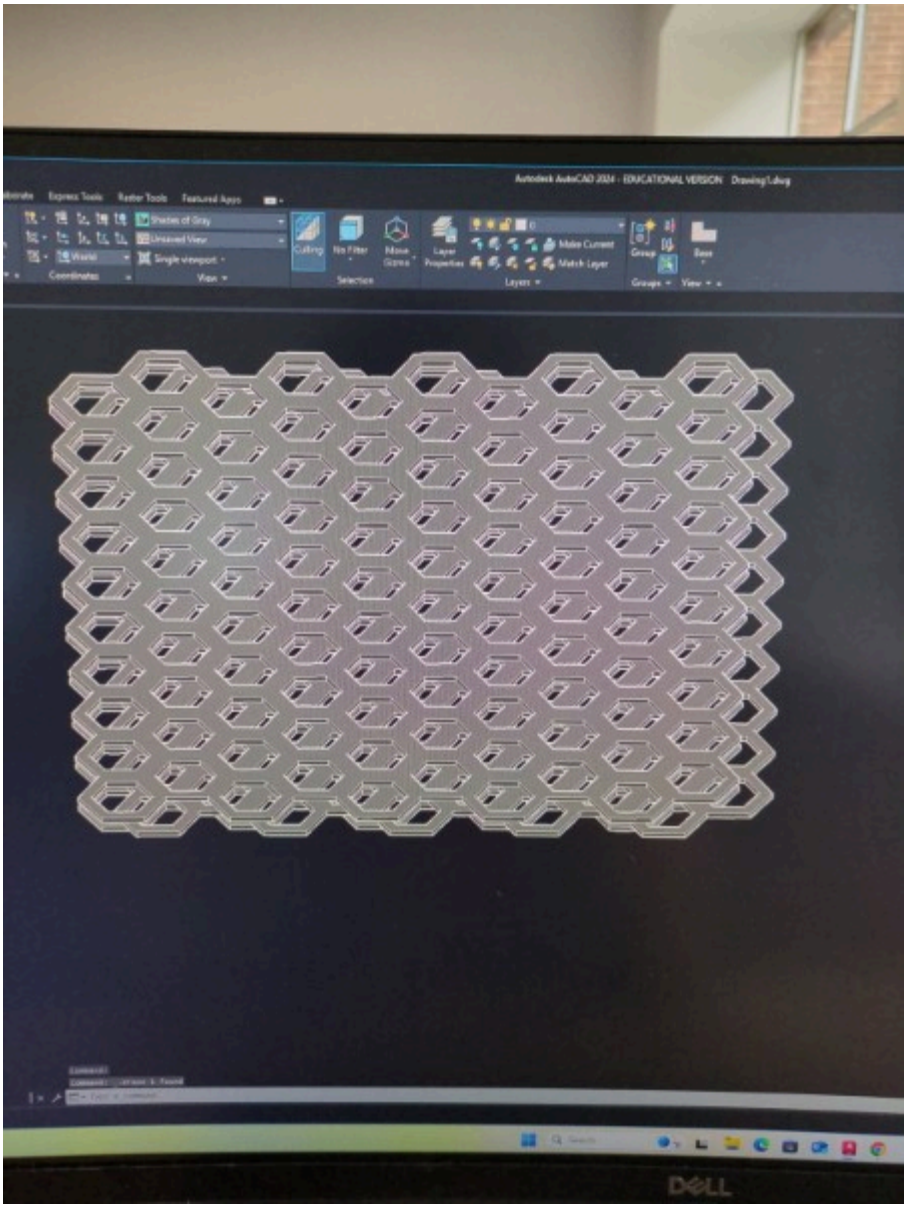

Figure 2: Hexagonal 3D-printed Scaffold model

Simulation:

We initially worked to develop an internal computational fluid dynamics (CFD) simulation in ANSYS Fluent for the scaffold model designed by our team. The simulation would focus specifically on the internal flow behavior through the scaffold structure, with the scaffold treated as a static and non-deforming body. No external flow conditions are applied around the scaffold, as our primary objective is to analyze how fluid motion is influenced within and across the porous scaffold geometry itself, rather than modeling the full complexity of flow that would occur within a blood vessel or arterial environment.
At this stage, our primary challenge lied in the mesh generation process. Due to the intricate nature of our scaffold geometry—with numerous small features, narrow passages, and fine edges—it proved difficult to establish a sufficiently quality mesh suitable for defining accurate flow parameters. The complexity of the

geometry makes it challenging to isolate the fluid domain and ensure adequate element resolution without incurring excessive computational costs.
Once the mesh generation issues were resolved, the remainder of the simulation setup—such as applying boundary conditions, initializing the flow field, and running the solver—would have proceeded relatively quickly. The main objective of this simulation is to visualize and analyze streamline patterns and mass flow rates throughout the scaffold structure. By doing so, we aimed to gain insight into how the scaffold geometry may influence local flow distribution, velocity gradients, and the overall flow resistance, thereby informing how such a scaffold could impact blood flow characteristics in potential biomedical applications. Below are properties of blood that we planned on using in defining our fluid, and a screenshot of our geometry that we worked on preparing for mesh.

Density	1069 kg/m^3
Dynamic Viscosity	2.78 mpa*s
Kinematic Viscosity	2.65 mm/s^s

Table 2: Fluid Properties of Blood at 37 ℃:

Ansys Mesh Geometry:

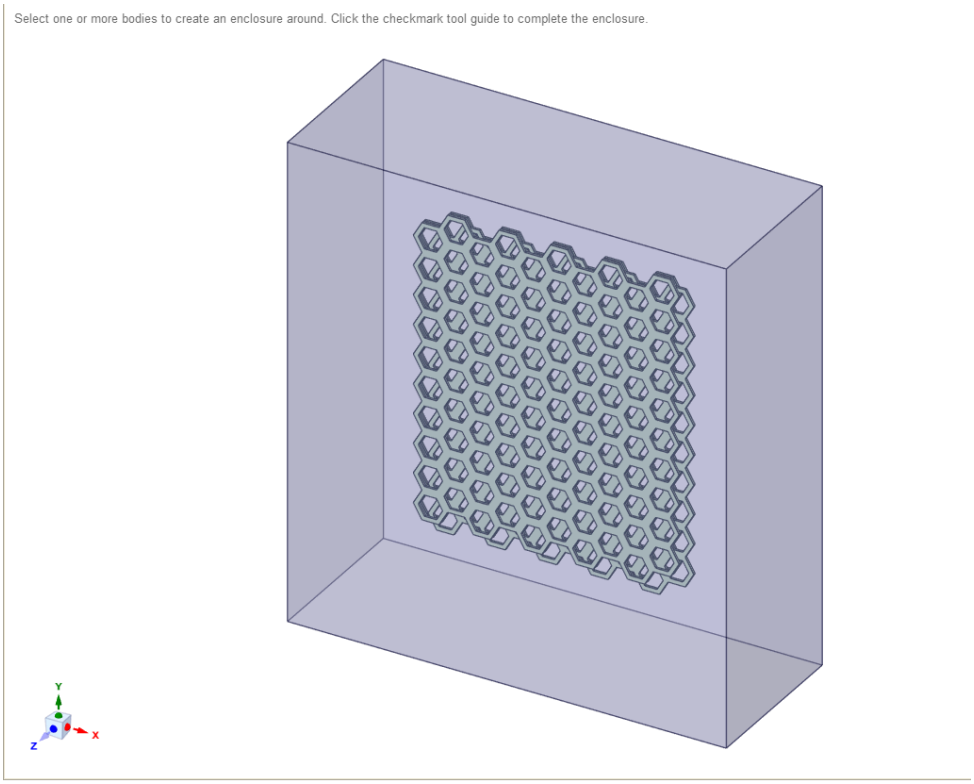

Figure 3: Mesh Geometry analysis

However, due to complications encountered with the fluid-based simulation and our limited prior experience with computational fluid dynamics (CFD), we chose to redirect our focus toward a structural analysis of the scaffolding model. This revised approach centers on evaluating the mechanical integrity of the structure under loading conditions comparable to those experienced during facial reconstruction applications. Since one of the most common biomedical uses for polymer scaffolding is in maxillofacial reconstruction, we based our loading parameters on the average human bite force, which typically ranges between 160 and 200 psi.

In this analysis, we aim to determine the resulting deformation, internal stresses, and potential points of failure when the model is subjected to shear forces within this range. The results will help assess the viability of polylactic acid (PLA) as a 3D-printed material for biomedical scaffolding under realistic physiological loads. For this simulation, the applied force will act tangentially along the surface of the scaffolding structure to generate shear stress, allowing us to evaluate how the material behaves under lateral loading conditions rather than purely compressive ones.

Below is the current version of our mesh as we continue to refine our setup:

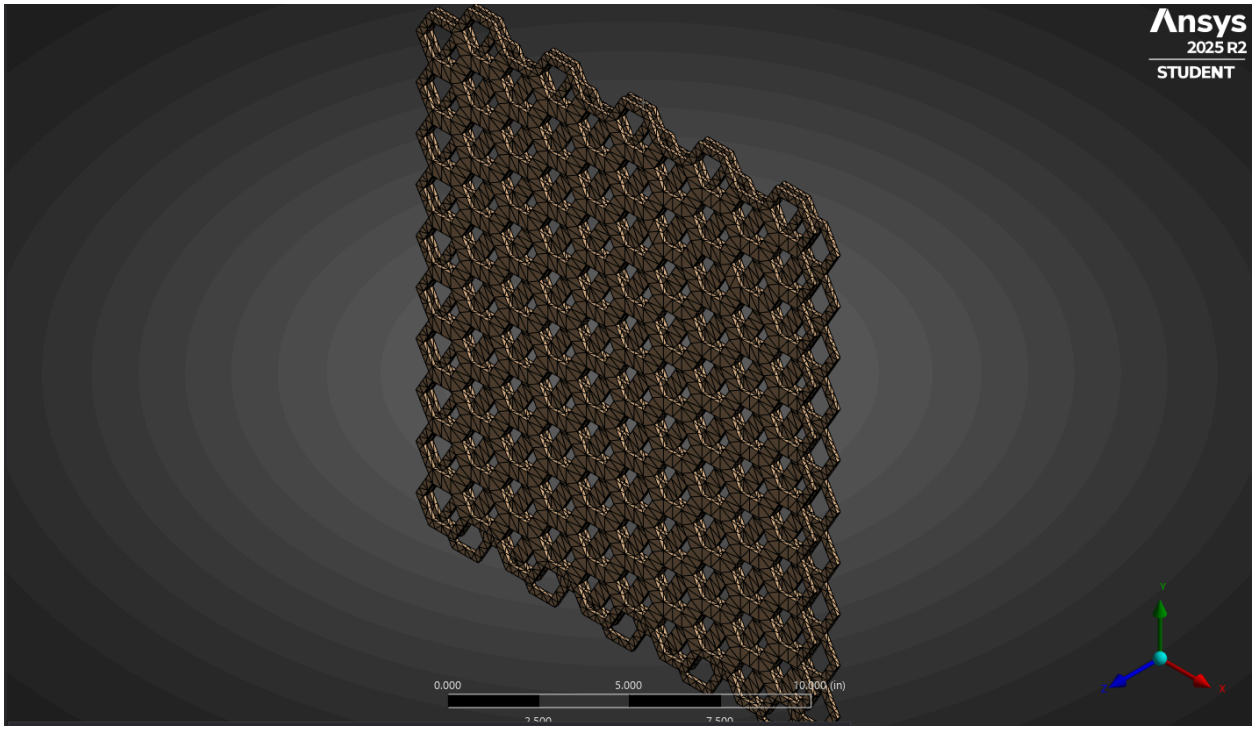

Figure 4: Refined Mesh 3D scaffold

Final Simulation Results:

Based on several key assumptions, the simulation was configured to model the mechanical forces on the scaffold. The sides of the structure were treated as fixed supports to define its boundary conditions. Since the complete material properties for the PLA filament were unavailable, the model used steel as a substitute; to compensate for this material discrepancy, the applied pressure vector was scaled by a factor equal to the ratio of the Young's moduli of PLA to steel. Furthermore, the forcing pressure vector itself was derived from an average human bite force, for which a conversion value of 140 pounds per square inch was applied in the simulation. As seen in the figures below, the maximum deformation value is 0.00018456 inches and the maximum von mises stress is 1.2652*10^5 psi.

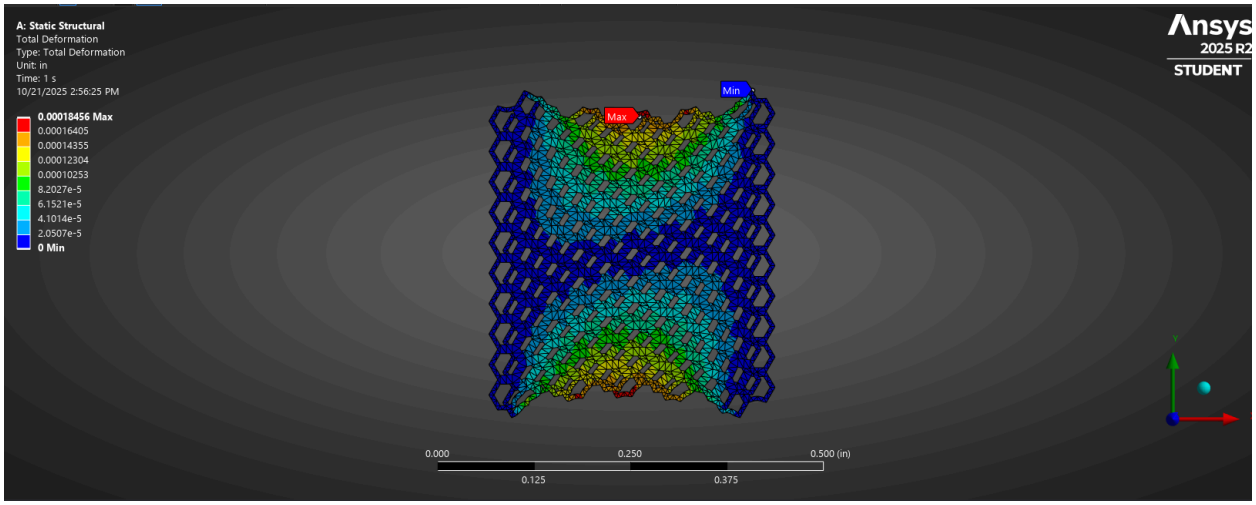

Figure 5: Final Mesh Deformation

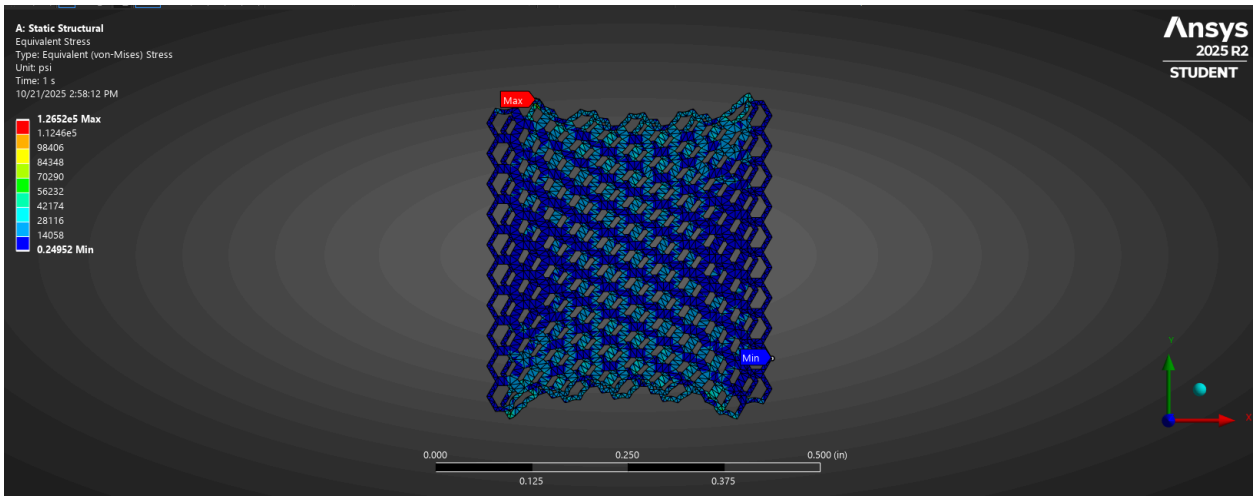

Figure 6: Equivalent Stress Scaffold Mesh

Conclusion:

The simulations show a structural analysis of the scaffold, which demonstrated little deformation under human bite pressure, that therefore validates the scaffold's practical utility. Rather than needing to be able to resist the entire load of the bite on its own, it provides structure for the tissue that is being formed in between the gaps and will provide additional support. The amount of deformation for PLA in the simulation is shown to be little enough to show how it would help patients to return functionality to their lives much earlier than otherwise would be possible. This low deformation would indicate that using an inexpensive and easily printable material like PLA could be used in medical scaffolding to great success, which could give widespread access to this technology. However, to ensure safety, we would suggest a denser grid which would more

evenly distribute the pressure in the scaffolding. The grid which was simulated had a very high maximum von mises value, well above the compressive strength of PLA (~13000 psi). While the testing conditions may have contributed to this high value, we would advise a higher-strength structure to be safe and prevent breakages and potentially worse conditions for patients. Overall, our simulations proved 3d printed medical scaffolding to be a promising upcoming technology for future development, even with lower strength materials such as PLA and other polymers.

Timeline/Gantt chart (References progress check):

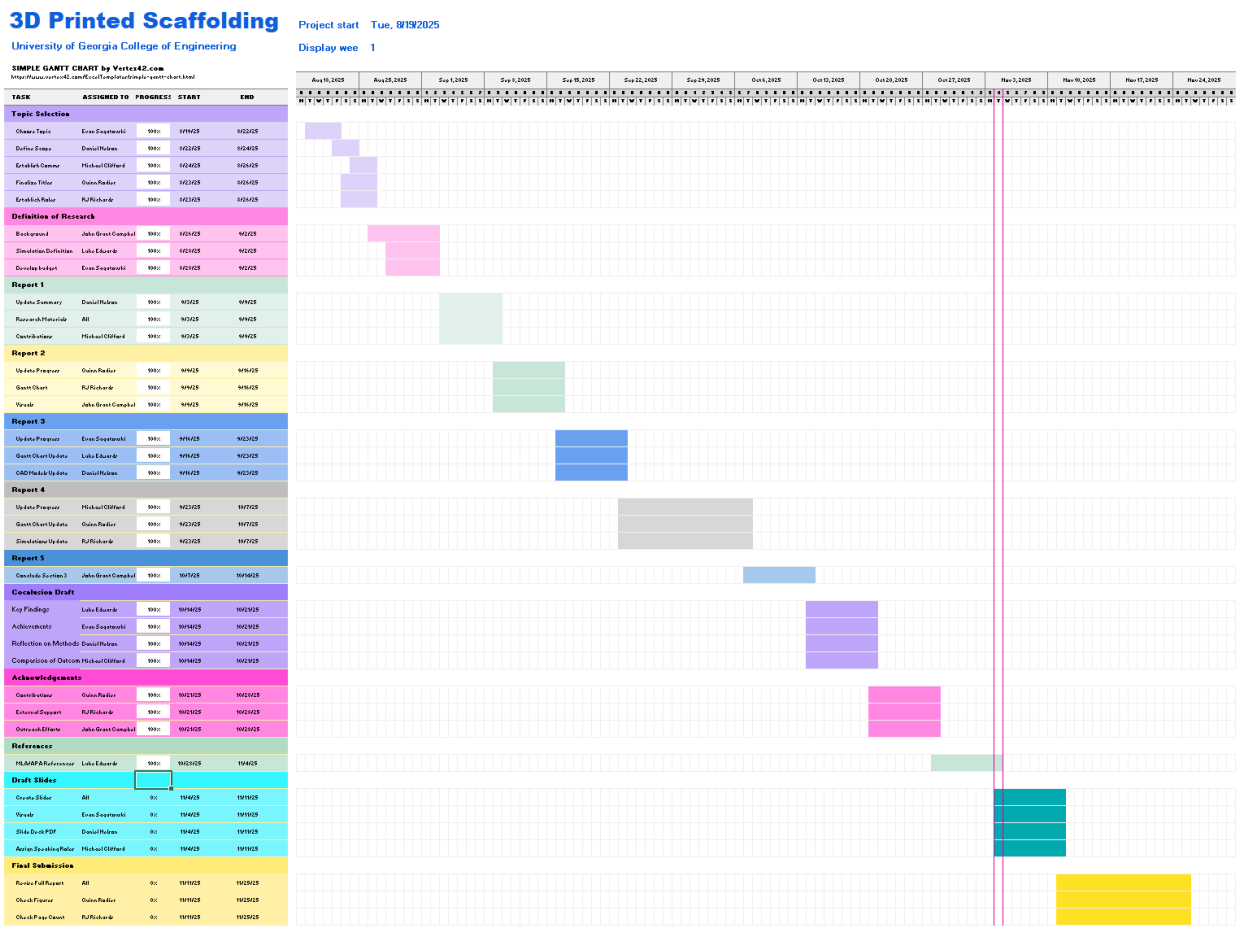

Acknowledgement

Evan Sagatovski	**Formatted Paper, wrote the introduction and abstract, author list, and references**
Quin Rodier	**Worked on the Mesh Analysis and Modeling of the original 3D scaffolds for the simulation, references**
Randal Richards	**Conducted the Studies and material tests, references**
Micheal Clifford	**Used Ansys for the Simulation of the 3D scaffolds to see the strength, references**
John Grant Campbell	**Worked on the conclusion, references**
Luke Edwards	**Updated the Gantt chart throughout the whole semester, and analyzed the data for the conclusion, references**
Daniel Nelson	**Main Researcher for the material use of the scaffold, worked on the background of the paper, references**

References

1. Chaudhuri, R., et al. “Additive Manufacturing in Tissue Engineering: Current Perspectives and Challenges.” *Materials Science and Engineering: C*, vol. 103, 2019, pp. 1251–1260.
2. Dorozhkin, Sergey V. “Calcium Orthophosphate-Based Biocomposites and Hybrid Biomaterials.” *Journal of Materials Science*, vol. 44, no. 19, 2009, pp. 4781–4855.
3. Farah, Shady, et al. “Physical and Mechanical Properties of PLA, and Their Functions in 3D Printing.” *Advanced Drug Delivery Reviews*, vol. 107, 2016, pp. 367–392.
4. Geetha, M., et al. “Ti Based Biomaterials, the Ultimate Choice for Orthopaedic Implants—A Review.” *Progress in Materials Science*, vol. 54, no. 3, 2009, pp. 397–425.
5. Hollister, Scott J. “Porous Scaffold Design for Tissue Engineering.” *Nature Materials*, vol. 4, no. 7, 2005, pp. 518–524.
6. Murphy, Sean V., and Anthony Atala. “3D Bioprinting of Tissues and Organs.” *Nature Biotechnology*, vol. 32, no. 8, 2014, pp. 773–785.
7. O’Brien, Fergal J. “Biomaterials & Scaffolds for Tissue Engineering.” *Materials Today*, vol. 14, no. 3, 2011, pp. 88–95.
8. Rajesh, P., et al. “Recent Advances in Carbon Fiber Reinforced Polymer Composites for Biomedical Applications.” *Biomaterials*, vol. 267, 2021, Article 120870. *ScienceDirect*,
9. Turnbull, G., et al. “3D Bioactive Composite Scaffolds for Bone Tissue Engineering.” *Bioactive Materials*, vol. 3, no. 3, 2018, pp. 278–314.
10. Wang, Xiaohong, et al. “Engineering Porous Scaffolds for Flexible Tissue Regeneration.” *Advanced Healthcare Materials*, vol. 2, no. 3, 2013, pp. 390–417.
11. Woodruff, Maria A., and Dietmar W. Hutmacher. “The Return of a Forgotten Polymer—Polycaprolactone in the 21st Century.” *Progress in Polymer Science*, vol. 35, no. 10, 2010, pp. 1217–1256.